Journal of
Mechanics of
Materials and Structures

A PROPOSED METHOD FOR FATIGUE CRACK DETECTION AND MONITORING USING THE BREATHING CRACK PHENOMENON AND WAVELET ANALYSIS

Viet Khoa Nguyen and Oluremi A. Olatunbosun

Volume 2, Nº 3 March 2007

mathematical sciences publishers

JOURNAL OF MECHANICS OF MATERIALS AND STRUCTURES
Vol. 2, No. 3, 2007

A PROPOSED METHOD FOR FATIGUE CRACK DETECTION AND MONITORING USING THE BREATHING CRACK PHENOMENON AND WAVELET ANALYSIS

VIET KHOA NGUYEN AND OLUREMI A. OLATUNBOSUN

In this paper the dynamic behavior of a fatigue cracked beam is investigated. The purpose is to reveal the nonlinear behavior of the structure with fatigue damage by using wavelet transform. A cracked cantilever beam is modeled by the finite element (FE) method using ALGOR™ software. A breathing crack is described in the FE method as a surface to surface contact of the two edges of the crack during vibration. Strain time history in the area adjacent to the crack has been analyzed using data processing techniques. Nonlinear effects in signals are usually difficult to detect by conventional data processing methods such as fast Fourier transform. However wavelet transform has recently been shown to be an effective method of detecting such nonlinear effects in signals. Modulus maxima, an important property of wavelet transform, have been used as an indicator of the crack size. Numerical results obtained from the FE analysis are presented in this paper, as well as some experimental results. It is shown that detection of fatigue cracks using breathing behavior and wavelet transform can be used to develop a vibration-based crack detection technique.

1. Introduction

Fatigue cracks of a structural member often occur after a period of loading cycles. This leads to structural failure. For this reason, methods of detecting and localizing cracks have been the subject of intensive investigation in the last two decades. In these methods, nondestructive methods for crack detection that are based on the changes in the dynamic properties of the structure caused by damage have been developed as an important tool for early detection of imminent failure in mechanical and civil engineering structures.

There are two main categories of crack models used in the methods: open crack models and breathing crack models. Most researchers have assumed that the crack in a structural member is open and remains open during vibration. This assumption was made to avoid the complexity resulting from nonlinear behavior when a breathing crack is presented. Nevertheless, during vibration, a crack will open and close due to an externally applied loading. During the vibration of a structure, edges of the crack come into and out of contact, leading to sudden changes in the dynamic response of the structure. This phenomenon is known as the breathing process of the crack. By introducing the concept of a breathing crack, an intensive investigation can reveal small changes in the dynamic response of the cracked element. These changes in dynamic response can be useful for detection of cracks.

Keywords: crack detection, crack monitoring, fatigue crack, breathing crack, closing crack, wavelet transform, wavelet analysis.

Nash [1969] investigated the dynamic response of a cracked beam under impact load. In this research, the governing equation of a cracked beam was derived with the aid of a variational principle developed by Gurtin [1964]. The governing equation was then solved by the approximate method known as the *small increment method* presented by Timoshenko [1913]. Carlson [1974] and Gudmundson [1983] studied the influences of closing cracks on the dynamical characteristics of a cracked cantilever beam. The relative increase in natural frequencies due to the closing crack phenomenon has been found to be much smaller than the decrease due to an open crack. Closing cracks in beams have been investigated by Chen and Chen [1988], Actis and Dimarogonas [1989], and Collin et al. [1992] in terms of nonlinear behavior of the longitudinal free and forced vibration using direct numerical integration. Kisa and Brandon [2000] studied the effects of closure of cracks on the dynamics of a cracked cantilever beam using successive modal transformations. Xastrau [1985] used the finite element method to study the steady state responses of a simply supported beam with multiple closing cracks. Matveev and Bovsunovsky [2002] investigated nonlinear distortions of the vibration characteristics due to fatigue damage. In their studies, the level of nonlinear distortions of the displacement, acceleration and strain waves of the cracked beam were studied and the comparative evaluation of their sensitivity was carried out using a successive algorithm (cycle by cycle). The Euler–Bernoulli beam model is used widely for breathing crack studies, but not the Timoshenko beam model. This is because the Timoshenko model is much more complicated when the effects of shearing deflection and rotational inertia are taken into account [Timoshenko and Young 1955]. However analytical results of the two models are the same for general slender beams [Kikidis and Papadopoulos 1992]. The existence of nonlinear dynamic behavior due to a breathing crack was proved by these authors. They related the breathing crack to changes in natural frequency and mode shapes. However they were not able to establish practical methods of detecting a crack using the changes in frequency and mode shapes because of the difficulty in detecting minute changes in frequency and mode shapes.

On-line methods for crack detection are preferred to other methods because they do not require the test to be stopped for inspection of the test specimen for damage during testing, thus providing considerable saving in time and cost. Most of these on-line methods are based on changes in dynamic characteristics of the object, for example, frequencies, mode shapes, transfer functions, and so on. In the field of signal processing, Fourier transform has been very useful and has been widely applied for a long time. However, when transforming a signal from the time domain (or space domain) into the frequency domain using Fourier transform, the time (or space) information is lost so that it is impossible to examine simultaneously the time and frequency characteristics of an event. Moreover, Fourier transform mainly works with stationary signals, while in practice many signals appear in the form of nonstationary signals. To overcome this shortcoming of the original Fourier transform, some signal processing methods based on Fourier transform have been developed. For example, short-time Fourier transform (STFT) was proposed by Gabor [1946]. By this method, the transformed signal can retain some information in the time domain. Nevertheless, this information is less precise when only one constant window is applied to the whole data set.

The wavelet transform method, like STFT, analyzes the signal in two dimensions: time (or space) and frequency. Instead of using only a constant width window as in STFT, wavelet transform uses a variable parameter called scale. The scale in wavelet transform can play a role similar to frequency in STFT. Because of this, wavelet transform is able to analyze signals locally. From its wavelet transform,

hidden details or irregular changes in a signal could be revealed efficiently. The vibration signal of a damaged structure might contain irregular events, thus, damaged structures could be examined by wavelet transform.

Ovanesova and Suarez [2004] used wavelet transform to analyze the deflection of an open cracked beam. The position of the crack was found using bior6.8 wavelet. These authors have also developed the method for application to frame structures and obtained satisfactory results. Douka et al. [2004] presented a method for crack identification in plates based on wavelet analysis. The crack is considered to be open. The position of the crack is determined by the sudden change in the spatial variation of the transformed displacement response. To estimate the depth of the crack, an intensity factor is defined which relates the depth of the crack to the coefficients of the wavelet transform. However, there are practical difficulties in applying these methods since they are based on minute changes in mode shapes or deflections which are very difficult to measure in practice. Also, a large number of transducers are required for such measurement. Furthermore, the assumption of open cracks may be inaccurate as many fatigue cracks are breathing cracks in practice.

In brief, the existence of breathing cracks has been proved by a series of papers. Some authors have tried applying the breathing crack phenomenon in order to detect cracks but it is still complicated or difficult to deploy in practice. Crack detection using wavelet transform is mainly based on the change of mode shapes of the structure after it is damaged but the practical measurement of mode shapes of structures is not easy.

In this paper a new approach, using a combination of the nonlinear behavior of a cracked beam during vibration and wavelet transform to detect cracks is presented. For this approach, the signal that needs to be measured to detect the crack is simple: the strain time history at one point close to the crack position. When a crack appears under load, based on the breathing crack phenomenon, strain time history will include distortion during subsequent dynamic loading. Therefore application of wavelet transform to the strain time history signal provides a means of monitoring the appearance of a crack and its depth.

2. Breathing crack

Consider a cracked Euler–Bernoulli cantilever beam as in Figure 1. Free bending vibration of a beam is described by the differential equation

$$\frac{\partial^4 z(x,t)}{\partial x^4} + \frac{\rho A}{EI}\frac{\partial^2 z(x,t)}{\partial t^2} = 0, \tag{1}$$

where E is the Young's modulus, ρ is the material density of the beam, A and $I = bh^3/12$ are the cross section area and inertia moment, respectively, and b and h are the width and the height of the cross section, respectively.

The solution of Equation (1) is written in the form

$$z(x,t) = \sum_{i=1}^{\infty} w_i(x)(P_i \sin \omega_i t + R_i \cos \omega_i t), \tag{2}$$

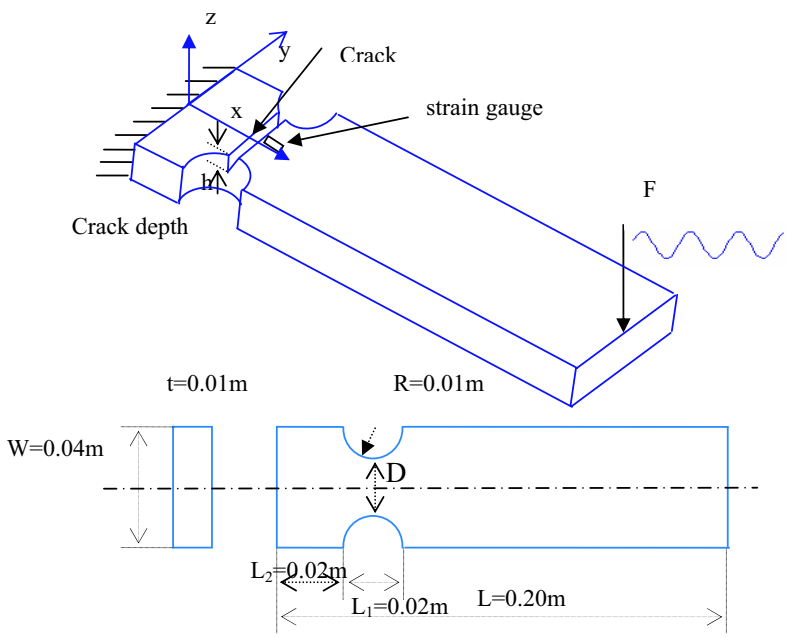

Figure 1. A cantilever beam with a crack.

where $w_i(x)$ is the i-th mode shape and ω_i is the i-th natural frequency. Mode shapes are expressed in the form [Matveev and Bovsunovsky 2002]

$$w_i(x) = A_i S(k_i x) + B_i T(k_i x) + C_i U(k_i x) + D_i V(k_i x), \tag{3}$$

where $k_i^4 = \frac{\omega_i^2 \rho A}{EI}$. S, T, U, and D are Krylov functions such that

$$S(x) = \sin(x) - \sinh(x), \qquad T(x) = \cos(x) - \cosh(x),$$
$$U(x) = \sin(x) + \sinh(x), \qquad D(x) = \cos(x) + \cosh(x).$$

The coefficients A_i, B_i, C_i, D_i can be calculated from the boundary conditions.

A cantilever with a crack can be modelled in sections. The crack is modeled by a short section with reduced cross section moment of inertia, while the sections on either side of the crack have the full cross section moment of inertia. For this model, the general solution of Equation (1) for the section j will be

$$z_{oj}(x,t) = \sum_{i=1}^{\infty} w_{ij}(x)(P_{oi} \sin \omega_{oi} t + R_{oi} \cos \omega_{oi} t), \tag{4}$$

and

$$w_{ij}(x) = A_{ij} S(k_{ij} x) + B_{ij} T(k_{ij} x) + C_{ij} U(k_{ij} x) + D_{ij} V(k_{ij} x), \tag{5}$$

where $w_{ij}(x)$ is the i-th mode shape of j-th section, and $k_{ij}^4 = \frac{\omega_{oi}^2 \rho A}{E I_j}$; $j = 1, 2$. The subscript o means the open crack.

A beam with a breathing crack is modeled as follows: at the half-cycles while the crack is closed, the vibrations of the beam are described by Equation (2) (with the assumption that there is no reduction of cross section at the crack position, this leads to the assumption that the stiffness of the intact beam and the stiffness of the beam with a closed crack are the same); at the half cycles while the crack is open, the vibration of the beam is described by Equation (4). Thus, the vibration of a cracked beam is described by a combination of Equations (2) and (4).

Matveev and Bovsunovsky [2002] presented the solutions of the vibration of the beam in two halves of one complete cycle with certain initial conditions as

$$z(x,t) = w_s(x)\sin\omega_s t, \tag{6}$$

$$z_{oj}(x,t) = P_{os}w_{sj}(x)\sin\omega_{os}t. \tag{7}$$

Solution (6) is the vibration of the beam in the first half-cycle with amplitude $w_s(x)$ and solution (7) is the vibration of the beam in the second half-cycle with amplitude $P_{os}w_{sj}(x)$, where s denotes the initial mode shape, and $P_{os} < 1$ and P_{os} is dependent on crack depth and material of the beam. Therefore, the amplitudes of the vibration of the beam are different in two halves of one complete cycle. This means that a breathing crack causes a distortion or singularity of the harmonic time functions, describing vibration characteristics such as displacement, strain, or acceleration. It is shown in [Matveev and Bovsunovsky 2002] that, for the different half cycles of vibration while the crack is closed or open, the normalized distribution function of strain along the beam length can be expressed as

$$\bar{\varepsilon}(x,t) = \bar{M}_s(x)\sin\omega_s t, \tag{8}$$

$$\bar{\varepsilon}_o(x,t) = f_\varepsilon(x,\gamma)P_{cs}\bar{M}_{sj}\sin\omega_{os}t, \tag{9}$$

where s signifies the initial mode shape, $f_\varepsilon(x,\gamma)$ is distortion function due to the crack's effect on strain distribution, and $\bar{M}_s(x)$ and $\bar{M}_{ij}(x)$ are normalized distribution functions of bending moment along the length of intact and cracked beams, respectively.

3. The wavelet transforms

Wavelet transform analysis uses a little wavelike function known as a wavelet. A more accurate description is that a wavelet is a function which has local wavelike properties. In mathematical terms, the wavelet transform is a convolution of the wavelet function with the signal. A wavelet transform is defined as [Daubechies 1992]

$$Wf(a,b) = \frac{1}{\sqrt{a}}\int_{-\infty}^{+\infty} f(t)\psi^*\Big(\frac{t-b}{a}\Big)\,dt, \tag{10}$$

where $f(t)$ is the input signal, a is a real number called scale or dilation, and b is a real number called position. $Wf(a,b)$ are wavelet coefficients of the function f, $\psi\big(\frac{t-b}{a}\big)$ is the wavelet function, and * denotes complex conjugation.

Let $\psi_{a,b}(t) = \frac{1}{\sqrt{a}}\psi^*\big(\frac{t-b}{a}\big)$. Equation (10) can be rewritten as

$$Wf(a,b) = \int_{-\infty}^{+\infty} f(t)\psi_{a,b}\,dt, \tag{11}$$

which describes the continuous wavelet transform (CWT). The CWT has an inverse transform:

$$f(t) = C_{\varphi}^{-1} \int_{-\infty}^{+\infty} \int_{-\infty}^{+\infty} Wf(a,b)\psi_{a,b}\, db\, \frac{da}{a^2}, \tag{12}$$

$$C_{\varphi} = 2\pi \int_{-\infty}^{\infty} \frac{|\hat{\psi}(\xi)|^2}{|\xi|}\, d\xi < \infty. \tag{13}$$

Modulus maxima. An important factor for detection of singularity are the local maxima of wavelet coefficients $Wf_{a,b}$, which are the local maxima of the derivative of $f(t)$ smoothed by $\phi(t)$. Mallat and Hwang [1992] presented a method using local maxima to detect singularity, and gave definitions as follows:

(i) Modulus maxima are points (a_0, t_0) such that $|C(a_0, t)| < |C(a_0, t_0)|$, when t belongs to either the right or the left neighborhood of t_0, and $|C(a_0, t)| \leq |C(a_0, t_0)|$ when t belongs to the other side of the neighborhood of t_0.

(ii) The maxima line is any connected curve in the scale space (a, b) along which all points are modulus maxima.

There is a connection of the regularity of a function at a point $t = t_0$ with the decay of the local maxima of the wavelet modulus across scales. To detect singularities, the asymptotic decay of the wavelet modulus maxima must be examined as the scale tends to zero. If the coefficients decay at the same rate as the scale decreases to zero, then t_0 is a singular point of $f(t)$. According to Mallat,

$$\log_2(|Wf(a,b)|) \leq \log_2 A + h \log_2(a), \tag{14}$$

where A is a constant and h is the Lipschitz regularity of function or Lipschitz exponent [Mallat and Hwang 1992]. The Lipschitz exponent gives more precise information about the differentiability of a function. For example, a function is not differentiable at $t = u$ if $0 < h < 1$. Therefore, the Lipschitz exponent h characterizes the nature of the singularity of the function $f(t)$ at $t = u$. A and h can be easily calculated from the intercept and gradient of the straight line (14) that is the asymptotic line of the curve $\log_2(|Wf(a,b)|)$ versus $\log_2(a)$. It is important to note that the Lipschitz exponent h describes the type of a singularity, as will be shown in more detail in the next sections.

4. Phase shift distribution

4.1. ***Definition.*** The definition of phase shift distribution is as follows:

(i) During vibration, the difference phase between two strain time history signals at two points on a structure is called the phase shift.

(ii) For a set of points along the structure, a set of phase shifts between these points and one reference point is called the phase shift distribution.

Methods for calculating phase shift distribution differ depending on types of excitation. Here, we consider two types: harmonic and random excitation.

4.2. ***Phase shift under harmonic excitation.*** It is known that under harmonic excitation at one frequency, the response of a structure will be a harmonic function of the same frequency, generally with a phase shift. The calculation of phase shift between output and harmonic input signal is presented as follows [Elsden and Ley 1969]. Assuming that the input signal is $f(t) = A\sin\omega t$ and the output signal is $\sigma(t) = R\sin(\omega t + \phi)$, the integrator outputs are

$$\frac{1}{NT}\int_0^N R\sin(\omega t+\phi)\sin\omega t\cdot dt = \frac{1}{2}R\cos\phi = \frac{a}{2}, \tag{15}$$

$$\frac{1}{NT}\int_0^N R\sin(\omega t+\phi)\cos\omega t\cdot dt = \frac{1}{2}R\sin\phi = \frac{b}{2}, \tag{16}$$

where $R = \sqrt{(a^2+b^2)}$, and NT is the integration time of N cycles of the wave form of period T. Dividing (16) by (15) we have

$$\phi = \tan^{-1}\left(\frac{b}{a}\right). \tag{17}$$

For M signals $\{\sigma_i(t)\}$, and $i = 1 \div M$ corresponding to measurement points from 1 to M, we have M phase shifts with the reference as the input signal. If one signal, for example $\sigma_1(t)$, in $\{\sigma_i(t)\}$, is selected to be the reference signal, the phase shift distribution is defined as

$$\Phi = \{0,\ \phi_2-\phi_1, \phi_3-\phi_1, \ldots, \phi_M-\phi_1\}. \tag{18}$$

4.3. ***Phase shift under random excitation.*** For random excitation, the phase shift distribution can be obtained from the concept of frequency response function [Wirsching et al. 1995]. A frequency response function is a mathematical representation of the relation between the input and output of a linear time-invariant system. If $x(t)$ and $y(t)$ are the input and output signals, the transfer function for every frequency ω is written in the form

$$|H(j\omega)| = \frac{Y(j\omega)}{X(j\omega)}, \tag{19}$$

where $Y(j\omega)$ and $X(j\omega)$ are Fourier transforms of $x(t)$ and $y(t)$.

The phase shift for any frequency ω can be calculated as

$$\begin{aligned}\phi(\omega) &= \text{angular}\,[H(j\omega)]\\ &= \text{angular}\,[Y(j\omega)] - \text{angular}\,[X(j\omega)].\end{aligned} \tag{20}$$

If $y^*(t)$ is another output signal, the phase shift between $y^*(t)$ and $x(t)$ is

$$\begin{aligned}\phi^*(\omega) &= \text{angular}\,[H^*(j\omega)]\\ &= \text{angular}\,[Y^*(j\omega)] - \text{angular}\,[X(j\omega)],\end{aligned} \tag{21}$$

where Y^* is Fourier transform of $y^*(t)$, and H^* is frequency response function between $x(t)$ and $y^*(t)$. From (20) and (21), the phase shift between two output signals $y(t)$ and $y^*(t)$ is calculated as

$$\begin{aligned}\phi^*(\omega) - \phi(\omega) &= \text{angular}\,[H^*(\omega)] - \text{angular}\,[H(\omega)]\\ &= \text{angular}\,[Y^*(j\omega)] - \text{angular}\,[Y(j\omega)].\end{aligned} \tag{22}$$

Case	Crack depth (%)
1	0
2	10
3	20
4	30
5	40
6	50
7	60

Table 1. Seven cases with cracks of varying depths at crack position $x = 30\,\text{mm}$.

Similar to harmonic excitation situation, if we have M signals $\{\sigma_i(t)\}$ corresponding to measurement points from 1 to M, the phase shift distribution with reference to $\sigma_1(t)$ is defined as

$$\Phi = \{0,\ \phi_2 - \phi_1, \phi_3 - \phi_1, \ldots, \phi_N - \phi_1\}. \tag{23}$$

5. Numerical studies

5.1. ***Strain analysis.*** To analyze the dynamic response of a cracked beam, the ALGOR - finite element software was used. The crack is described as shown in Figure 1. In this model the crack includes two close edges. In ALGOR, a surface to surface contact tool is used in a mechanical event simulation (MES) to model the breathing crack. It is expected that when the load is a sinusoidal function, the strain function should not be completely sinusoidal, but should be distorted when the crack closes.

From the definition of a wavelet transform, Equation (10), it is obvious that wavelet coefficients are proportional to vibration amplitude. On the other hand, vibration amplitude of the beam is proportional to load amplitude. This leads to the fact that the distortion of strain is proportional to force level. For this reason, a normalization of strain time history is needed before data processing, to detect the level of the crack.

Seven levels of the crack from zero to 60% were examined. These seven cases are numbered as in Table 1. The two types of applied forces are harmonic and random functions.

5.2. *Detection of crack existence and crack depth using wavelet transforms.*

5.2.1. *Detection of crack existence.* The wavelet transforms were applied for analyzing strain-time signals at the point adjacent to the crack under dynamic load for seven levels of crack depth. The wavelet function used was db2, which is the Doubachives wavelet family with two vanishing moments. In this analysis, the discrete wavelet transform was applied. The original signal is strain time history.

Figures 2–5 describe strain-time history and its wavelet transform for specific levels of the crack. In each figure, the upper graph shows strain time history and the lower graph shows its wavelet transform. Obviously, the nonlinear phenomena of strain signals cannot be detected visually in all strain-time history graphs. To reveal the nonlinear phenomena caused by the appearance of the crack, wavelet transform is applied. As can be seen in the lower graphs, when there is no crack, or the crack depth is smaller than 30%, no discontinuity in the wavelet transform is shown. However, when the crack depth is equal or

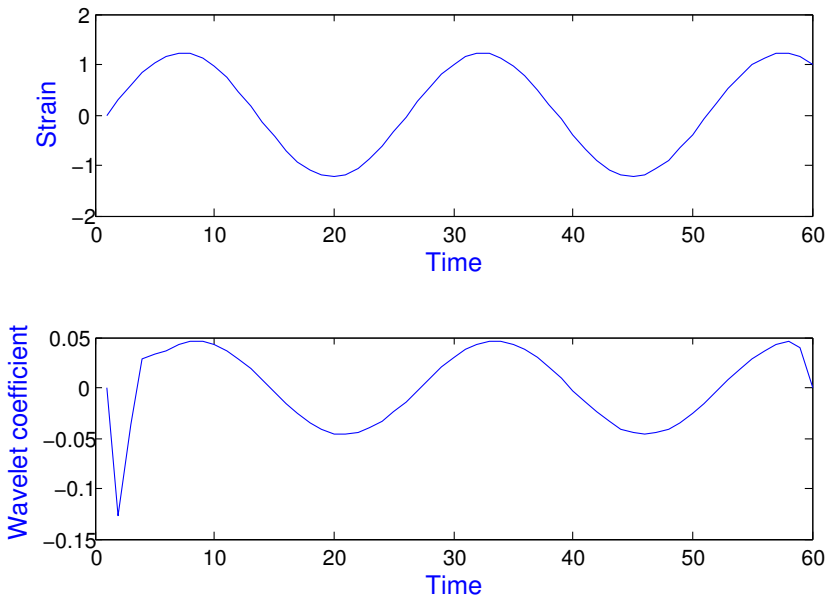

Figure 2. Intact specimen.

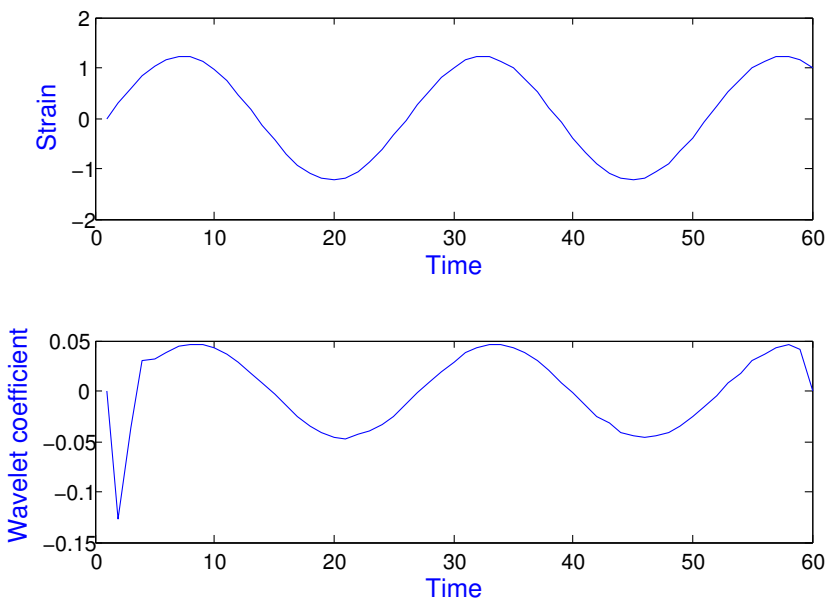

Figure 3. Specimen with 20% crack depth.

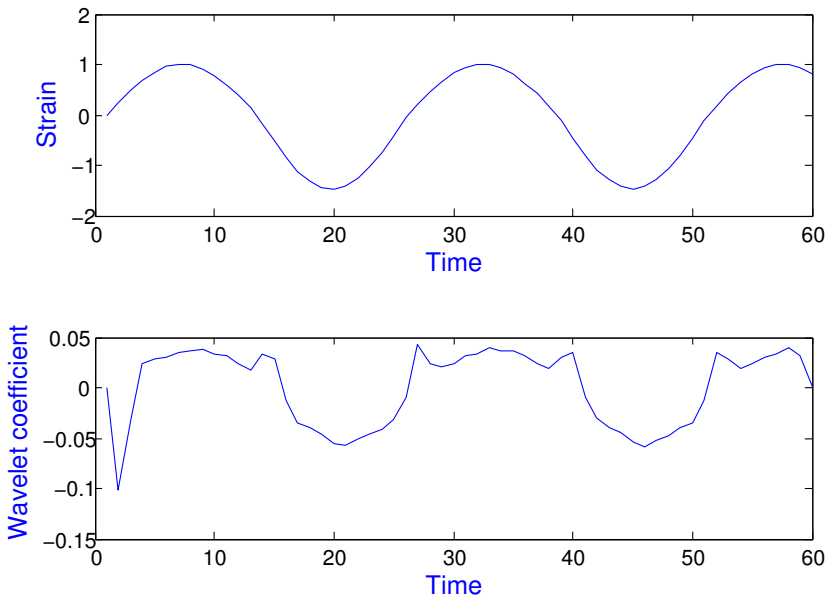

Figure 4. Specimen with 40% crack depth.

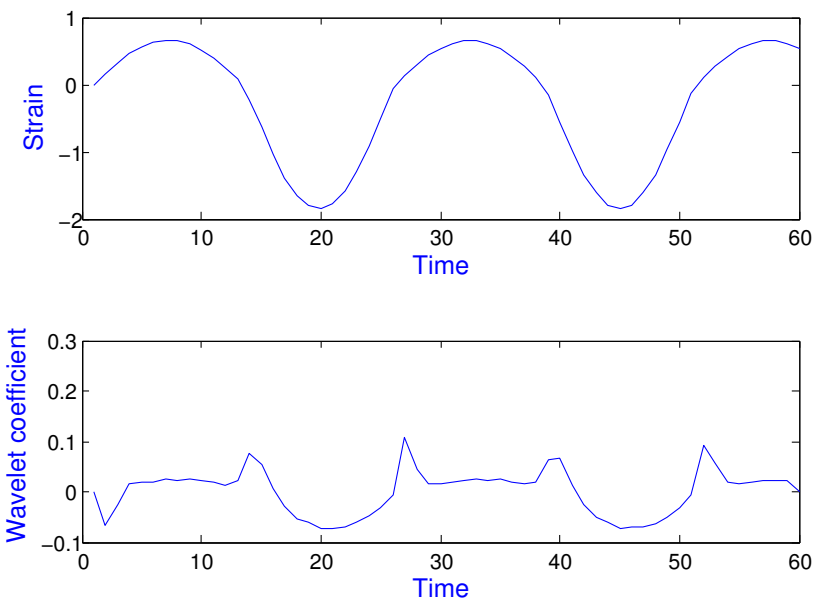

Figure 5. Specimen with 60% crack depth.

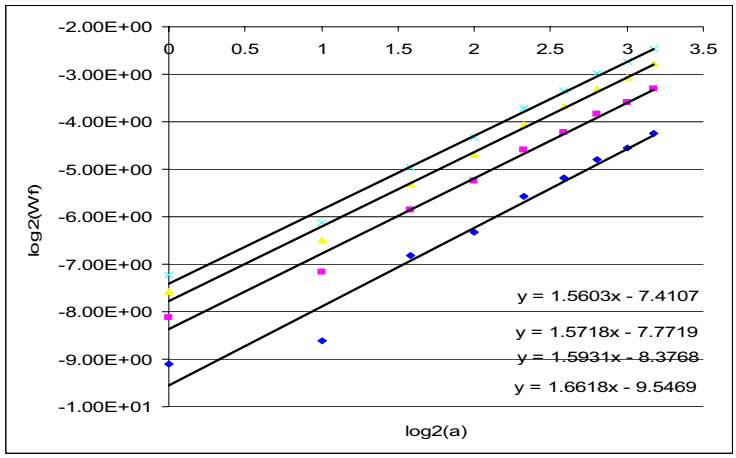

Figure 6. Maxima lines versus scale for five levels of crack: the lowest line is for the crack of 30% and the highest line is for the crack of 60%.

greater than 30%, the wavelet transform clearly shows discontinuities at moments when breathing of the crack occurs. These discontinuities of the wavelet transform indicate that the test specimen contains a crack.

5.2.2. *Detection of crack depth.* To determine crack depth, the modulus maxima lines of the wavelet transform have to be investigated. For this purpose, Equation (14) is used to describe the relationship between crack depth and the coefficients of the wavelet transform.

As can be seen in Figure 6 the wavelet maxima lines versus scale are shown for crack depths varying from 30 % to 60% of the wavelet transform. These four lines are parallel lines of the same slope, or in other words, of the same Lipschitz exponent. The Lipschitz exponent for all cases has a constant value of 1.6, which indicates that singularities of the same type are caused by the same physical process — in this case, the existence of a crack. From Figure 6, when the Lipschitz exponent h is fixed, only the intercept A changes when the crack depth changes. Thus, each parallel line can be distinguished by its intercept A. This intercept increases when crack depth increases. The intercept A therefore can be considered as an intensity factor which relates the extent of the fatigue crack to the wavelet coefficients.

Establishing a graph of intercept A versus crack depth from Figure 6, a relationship between intercept A (or intensity factor) and crack depth is obtained as shown in Figure 7. The values of A plotted are the linear values derived from the log-log plot in Figure 6. It can be seen that this relationship is the straight line in semilog plot. Because of this, Figure 7 can be used to predict the crack depth if the intensity factor is known.

5.3. ***Detection of crack position.*** A method of detection of crack position using phase shift distribution of strain signals along the structure is proposed. The idea is that the strain wave traveling along the beam might be influenced by a sudden change in its transmission direction, such as a crack. Therefore, a phase shift of the strain signal at points along the beam could be influenced as well and could be used to detect

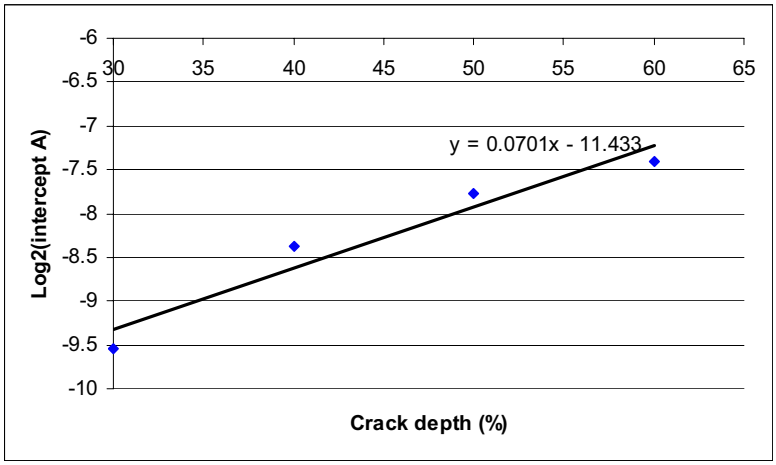

Figure 7. Intensity factor versus crack depth.

the position of the crack. Due to the existence of damage, the phase shift distribution of a damaged structure is expected to differ from that of an intact structure, at the position of the damage.

To investigate the phase shift distribution, six strain time history signals are obtained at six points, from finite element (FE) analysis as shown in Figure 8. The relative positions of the six points labeled from 1 to 6 are 0, 5.5, 10.6, 16.4, 22.7, and 28.7 mm, respectively. The crack position is between points 3 and 4, at a position of 13.5 mm.

5.3.1. *Detection of crack position using phase shift under harmonic excitation.* Figures 9–12 present phase shift distributions calculated from FE analysis results for the beam with increasing crack depth

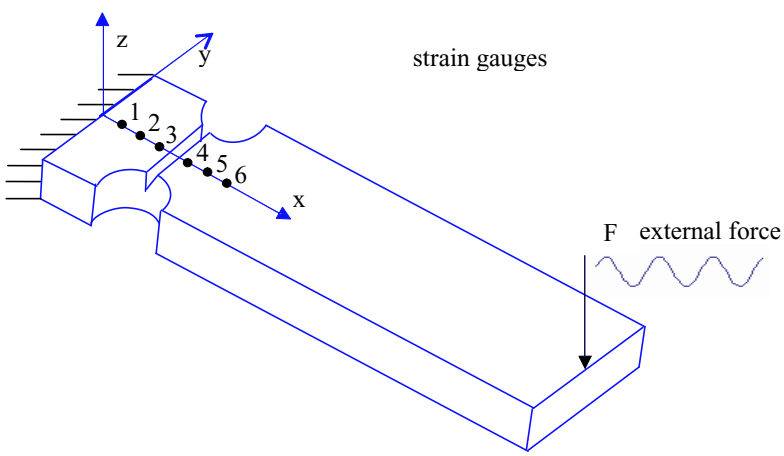

Figure 8. Positions of the six points along the beam.

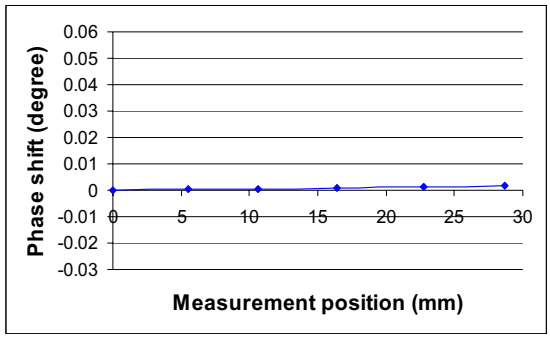

Figure 9. Phase shift distribution of the intact beam.

in the case of harmonic excitation. As can be seen in Figure 9, when the beam has no crack, the phase shift distribution is smooth. In Figure 10 when the crack depth increases to 20%, there is a distortion in the phase shift distribution at a position between point 3 and point 4. It is interesting that the shape of the distortion remains the same, and only the amplitude increases when the crack depth increases (see Figures 11 and 12).

From this result, it is obvious that the crack position can be detected as the position of the distortion in the phase shift distribution.

5.3.2. *Detection of crack position using phase shift under random excitation.* Figures 13–16 show phase shift distribution of the beam under random excitation for specific cases when crack depth increases from zero to 60%. The phase shift distribution is calculated at the resonant frequency.

Clearly, the shape and position of the distortion in phase shift distribution changes when the excitation and crack depth vary. This means that under random excitation, there is no rule to relate the position of the crack to the distortion of phase shift distribution. In other words, phase shift distribution cannot be used to detect the crack position under random excitation.

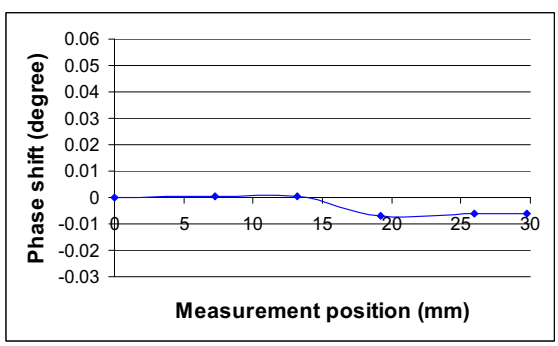

Figure 10. Phase shift distribution of the beam with crack of 20% depth.

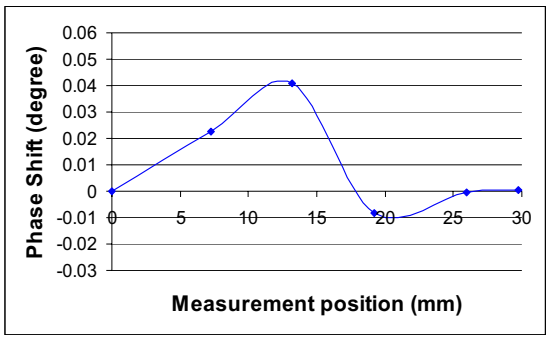

Figure 11. Phase shift distribution of the beam with crack of 40% depth.

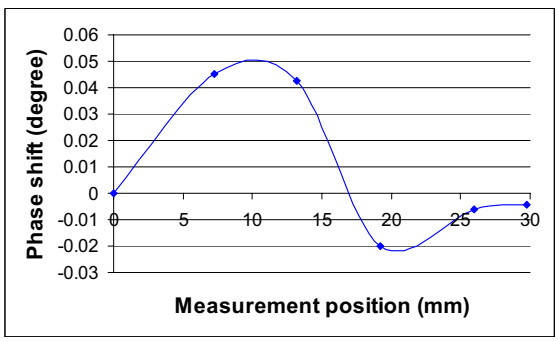

Figure 12. Phase shift distribution of the beam with crack of 60% depth.

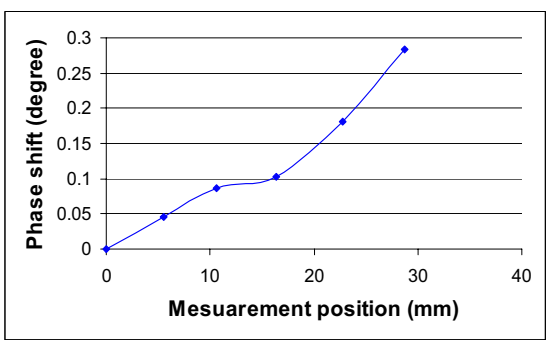

Figure 13. Phase shift distribution of the intact beam.

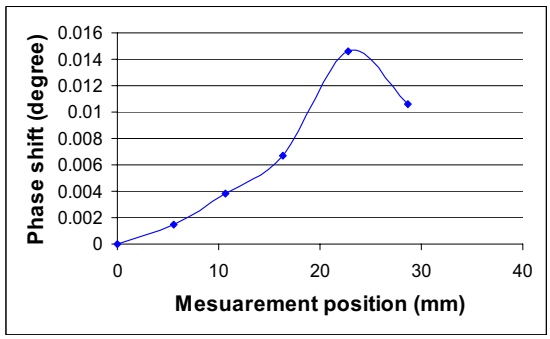

Figure 14. Phase shift distribution of the beam with crack of 20% depth.

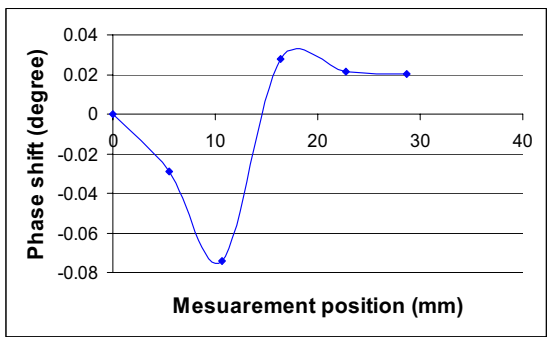

Figure 15. Phase shift distribution of the beam with crack of 40% depth.

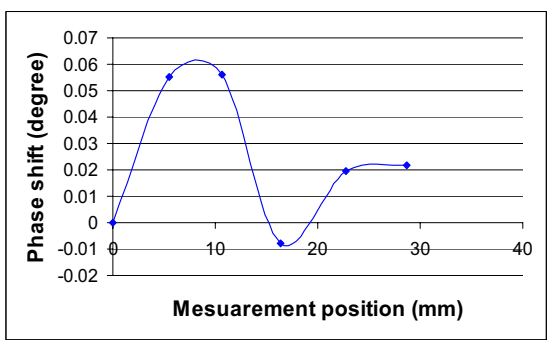

Figure 16. Phase shift distribution of the beam with crack of 60% depth.

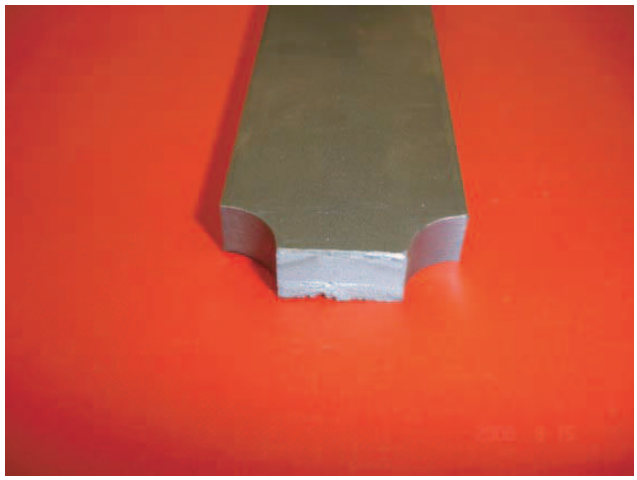

Figure 17. Crack shape of the specimen.

6. Experimental results

To validate the method for crack detection using the breathing crack model and wavelet analysis, fatigue tests on a cantilever beam have been carried out. A specimen made from mild steel BS970 was used, with a size similar to the beam in the FE model (see Figure 1). The excitation force was generated using an electro-hydraulic actuator and was controlled by LabView using a National Instruments device and Kelsey Instruments controller. Exciting frequency was 10 Hz. The crack shape obtained from experiment is quite similar to the numerical case: the crack line is fairly straight and edges of the crack are reasonably flat (see Figure 17).

6.1. ***Detection of crack existence.*** Figures 18–21 describe strain time history and its wavelet transform for six cases taken at different stages during the fatigue test on the specimen. In these figures, wavelet transform at level 2 and wavelet function db2 are applied.

Visually, the distortions in strain time histories caused by the crack are not apparent (see upper graphs in Figures 18–21). However, these distortions are highlighted from the wavelet transform (lower graphs in Figures 19–21). Figure 18 shows the measured strain and its wavelet transform for the specimen at the beginning of the test when no crack has yet developed. Obviously, there is no peak in the wavelet transform for this case. It means that when there is no crack, the wavelet transform does not give any information about the crack. As can be seen in Figures 18–21, when the crack is from 19% to 58%, the wavelet transforms show clear peaks. This indicates the presence of distortion in the strain time history and, hence a crack in the specimen. However, the peaks in wavelet transform of the measured signals are not as clean as in the FEM results. This can be explained by the background noise in the measured signals during testing, resulting from sources such as the electro-hydraulic pump and the exciter mechanism.

6.2. ***Detection of crack depth.*** Figure 22 shows a comparison of the relationship between crack depth and the intercept A in two cases: experimental and FE analysis. As can be seen in this figure, the relationship in semilog plot between crack depth and value of intercept A obtained from experimental

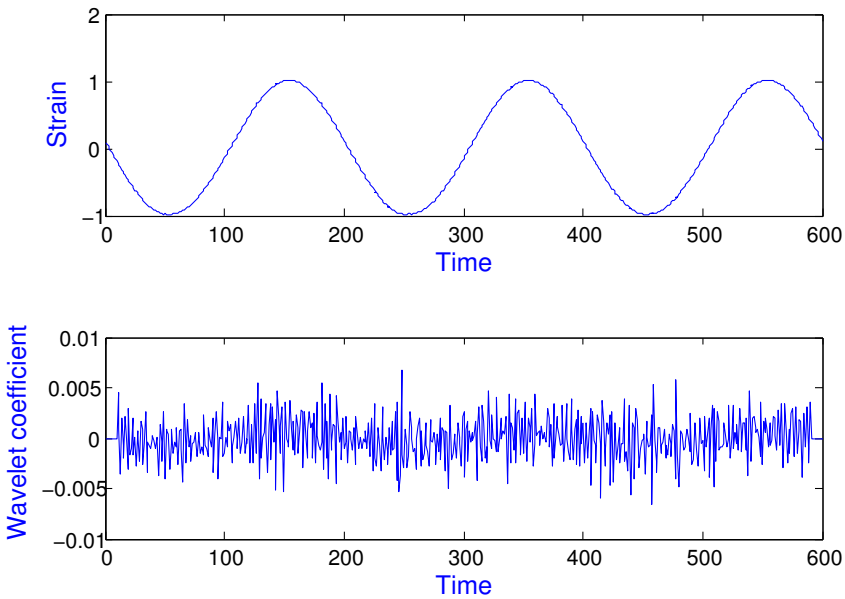

Figure 18. Strain and its wavelet transform; crack is 0%.

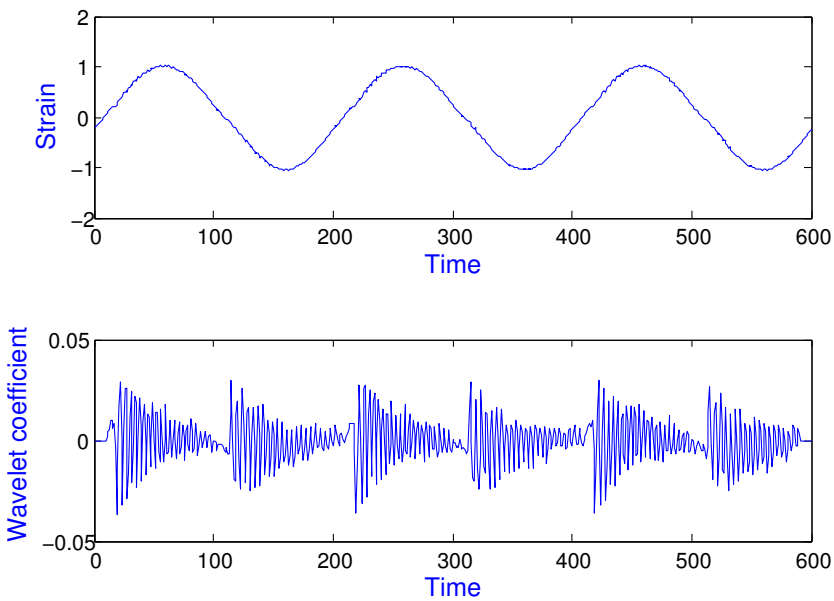

Figure 19. Strain and its wavelet transform; crack is 19%.

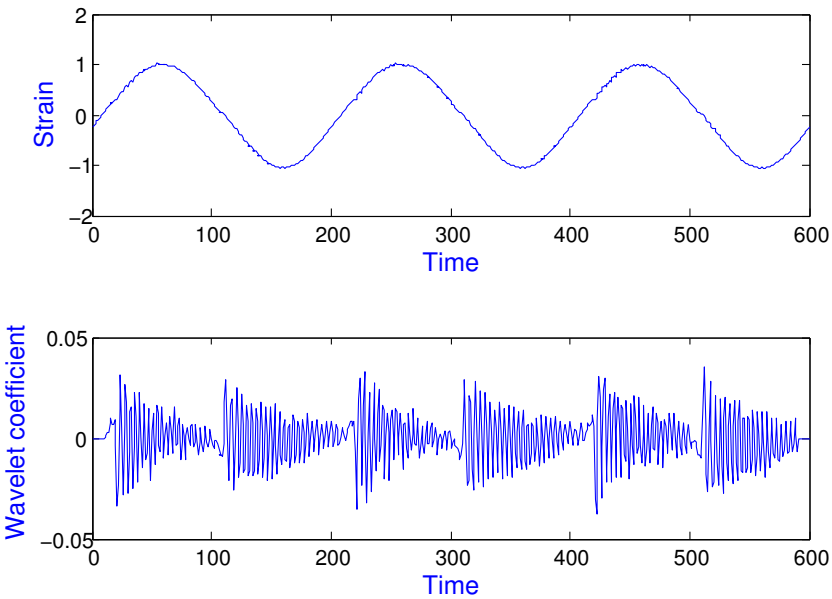

Figure 20. Strain and its wavelet transform; crack is 41%.

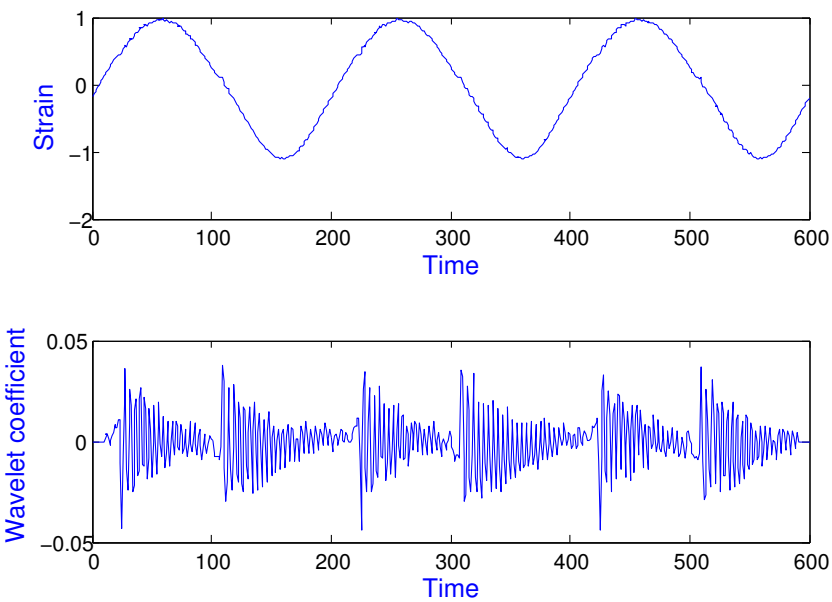

Figure 21. Strain and its wavelet transform; crack is 58%.

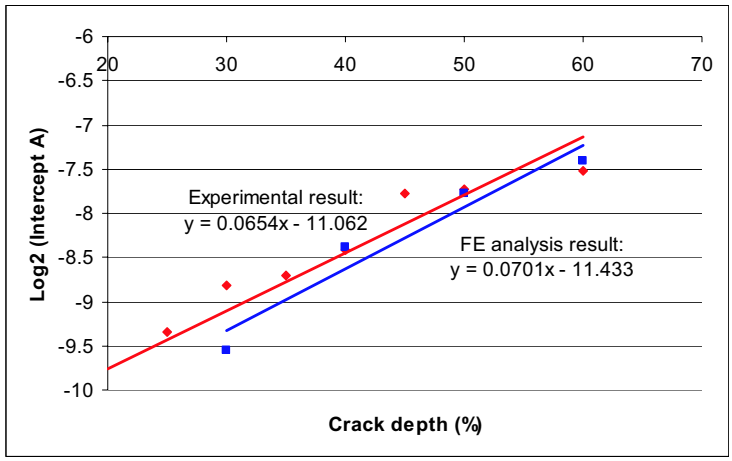

Figure 22. Relationship between crack depth and intercept. The red line is the experimental result, and the blue line is the FE analysis result.

results is linear. The intercept A increases when the crack depth increases. Note that there are still differences between numerical and experimental results. The Lipschitz exponent from the experiment is 1.0 and differs from FE analysis, where the value of the Lipschitz exponent is 1.6. This can be explained by the fact that the two edges of the crack do not come into contact purely, but rather the contact of these two edges may contain sticking, frictionless sliding, and friction sliding phenomena. On the other hand, the surfaces of two edges of a crack are not as smooth as when modeled in FE analysis. Background noise, as mentioned in Section 6.1, may also be a contributory factor to the difference between numerical and experimental results.

6.3. ***Detection of crack position.*** To measure phase shift distribution, four strain gauges are used. The relative positions of these points from 1–4 are 0, 17 , 25, and 46 mm, respectively. Three tests have been carried out and gave the same results. The actual crack position is found at 20 mm which means the crack is between point 2 and point 3. Figures 23–26 show the phase shift distribution for specific cases taken at different stages during the fatigue test on the specimen.

Figure 23 shows the phase shift distribution for the specimen at the beginning of the test when no crack has yet developed. As can be seen in this figure, the phase shift distribution when there is no crack is above the horizontal axis and quite smooth as expected. From Figures 24–26, when the crack for these cases is from 19% to 58%, the shapes of phase shift distributions remain the same while the distortion is found clearly at a position between point 2 and point 3. Thus, it can be said that the crack position is well detected by the phase shift distribution.

7. Conclusions

A method for crack detection in a beam based on the breathing crack phenomenon and wavelet transform has been presented. The appearance of the crack is detected by the singularities in strain time history caused by the breathing phenomenon of the crack. Such singularities are usually difficult to discriminate

visually. However, applying the wavelet transform has given clear pictures of these singularities. The relationship between crack depth and intensity factor was also determined. The linear relationship between crack depth and intensity factor in a semilog plot has been obtained in both numerical and experimental data.

A fatigue test with a simple specimen has been carried out in the laboratory. The experimental results are in agreement with the results of FE analysis in terms of detecting the appearance of the crack. When there is no crack or the crack depth is small, there is no discontinuity in the wavelet transform. Although the experimental signals were noisy, the appearance of the crack was detected quite clearly by peaks in the wavelet transform. The estimation of crack depth based on experimental data has been carried out. The relationship between crack depth and the intensity factor A is established. It is shown that the intensity factor (intercept A) increases when the crack depth increases. However, there is a significant difference in experimental results when compared with numerical analysis in terms of detecting crack depth, due to the influences of real conditions during the test.

A new approach based on phase shift distribution for the detection of crack position is also proposed. The position of the crack is accurately detected when the specimen is excited under harmonic load. The crack position is determined by the position of the distortion in phase shift distribution. The phase distribution has to be determined under harmonic excitation, as it has been shown that this technique does not work under random excitation.

To conclude, the method of combining the breathing crack phenomenon and wavelet transform is adequate to apply for monitoring the appearance of a crack in the test specimen. The nonlinearity resulting from the breathing crack phenomenon is clearly shown by wavelet transform of the strain time history. The advantages of this technique are that it is capable of being implemented in a practical manner, and the strain time history signal can be easily measured in practice. Also, the amount of measured data required for crack detection is easily manageable for the implementation of on-line crack detection and monitoring.

This paper has established the proposed technique for structural health monitoring using a simple structure. Further studies on real components under real test conditions are now in progress.

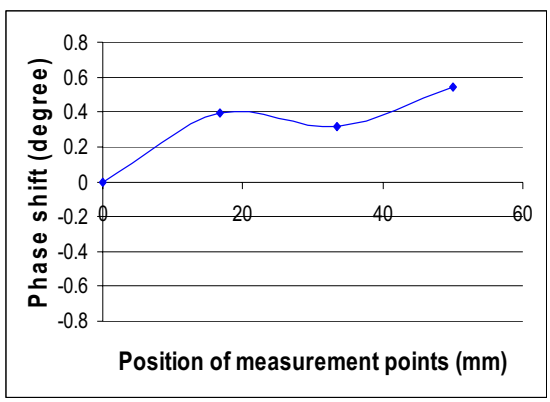

Figure 23. Phase shift distribution of the intact beam.

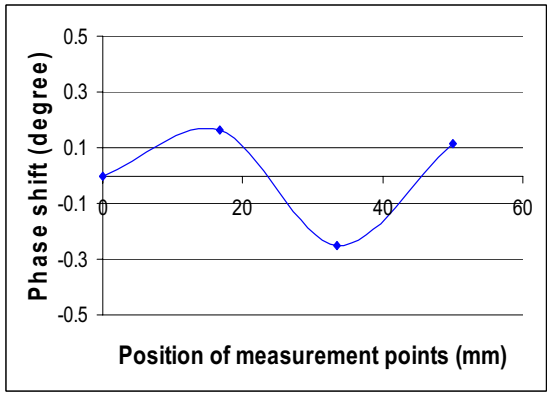

Figure 24. Phase shift distribution of the beam with crack of 19% depth.

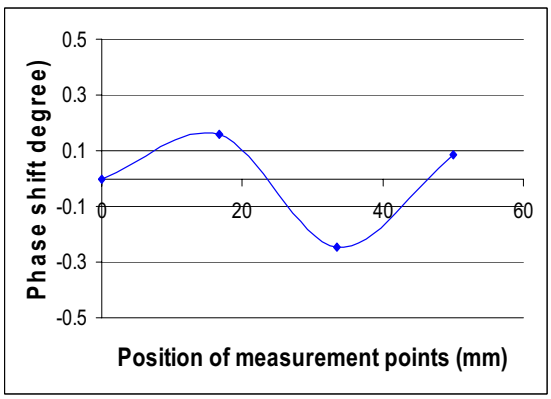

Figure 25. Phase shift distribution of the beam with crack of 41% depth.

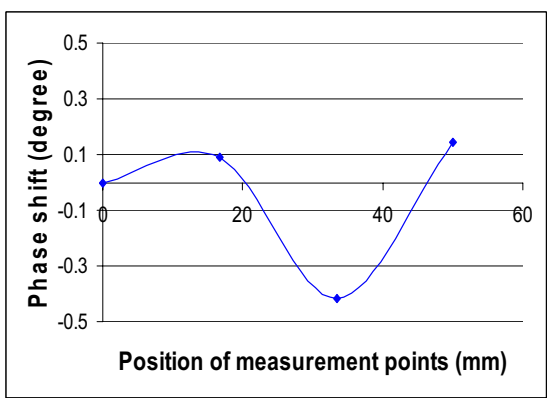

Figure 26. Phase shift distribution of the beam with crack of 58% depth.

References

[Actis and Dimarogonas 1989] R. L. Actis and A. D. Dimarogonas, "Non-linear effects due to closing cracks in vibrating beams", pp. 99–104 in *Structural vibration and acoustics: 12th Biennial Conference on Mechanical Vibration and Noise* (Montréal), edited by T. S. Sankar et al., ASME Design Engineering **18(3)**, ASME, New York, 1989.

[Carlson 1974] R. L. Carlson, "An experimental study of the parametric excitation of a tensioned sheet with a crack-like opening", *Exp. Mech.* **14**:11 (1974), 452–458.

[Chen and Chen 1988] L. W. Chen and C. L. Chen, "Vibration and stability of cracked thick rotating blades", *Comput. Struct.* **28**:1 (1988), 67–74.

[Collin et al. 1992] K. R. Collin, P. H. Plaut, and P. H. Wauer, "Free and forced longitudinal vibrations of a cantilevered bar with crack", *J. Vib. Acoust.* (*ASME*) **114** (1992), 171–177.

[Daubechies 1992] I. Daubechies, *Ten lectures on wavelets*, CBMS Regional Conference Series in Applied Mathematics **61**, SIAM, Philadelphia, 1992.

[Douka et al. 2004] E. Douka, S. Loutridis, and A. Trochidis, "Crack identification in plates using wavelet analysis", *J. Sound Vib.* **270**:1–2 (2004), 279–295.

[Elsden and Ley 1969] C. S. Elsden and A. J. Ley, "A digital transfer function analyser based on pulse rate techniques", *Automatica* **5**:1 (1969), 51–58.

[Gabor 1946] D. Gabor, "Theory of communication", *J. Inst. Elect. Eng.* **93** (1946), 429–457.

[Gudmundson 1983] P. Gudmundson, "The dynamic behaviour of slender structures with cross-sectional cracks", *J. Mech. Phys. Solids* **31**:4 (1983), 329–345.

[Gurtin 1964] M. E. Gurtin, "Variational principles for linear elastodynamics", *Arch. Ration. Mech. An.* **16**:1 (1964), 34–50. MR 35 #5173 Zbl 0124.40001

[Kikidis and Papadopoulos 1992] M. L. Kikidis and C. A. Papadopoulos, "Slenderness ratio effect on cracked beam", *J. Sound Vib.* **155**:1 (1992), 1–11.

[Kisa and Brandon 2000] M. Kisa and J. Brandon, "The effects of closure of cracks on the dynamics of a cracked cantilever beam", *J. Sound Vib.* **238**:1 (2000), 1–18.

[Mallat and Hwang 1992] S. Mallat and W. Hwang, "Singularity detection and processing with wavelets", *IEEE Trans. Inform. Theory* **38**:2 (1992), 617–643.

[Matveev and Bovsunovsky 2002] V. V. Matveev and A. P. Bovsunovsky, "Vibration-based diagnostics of fatigue damage of beam-like structures", *J. Sound Vib.* **249**:1 (2002), 23–40.

[Nash 1969] G. E. Nash, "Mechanical aspect of the dynamic tear test", *J. Basic Eng.* (*ASME*) **91** (1969), 535–543.

[Ovanesova and Suarez 2004] A. V. Ovanesova and L. E. Suarez, "Applications of wavelet transforms to damage detection in frame structures", *Eng. Struct.* **26**:1 (2004), 39–49.

[Timoshenko 1913] S. P. Timoshenko, "Zur Frage nach der Wirkung eines Stosses auf einen Balken", *Z. Math. Phys.* **62** (1913), 198–209.

[Timoshenko and Young 1955] S. P. Timoshenko and D. H. Young, *Vibration problems in engineering*, 3rd ed., Van Nostrand, New York, 1955.

[Wirsching et al. 1995] P. H. Wirsching, T. L. Paez, and K. Ortiz, *Random vibrations: theory and practice*, Wiley, New York, 1995.

[Xastrau 1985] B. Xastrau, "Vibration of cracked structures", *Arch. Mech.* **37** (1985), 731–743.

Received 20 Jun 2006. Accepted 23 Sep 2006.

VIET KHOA NGUYEN: nguyenvietkhoa_vc@yahoo.com
School of Mechanical Engineering, The University of Birmingham, Edgbaston, Birmingham B15 2TT, United Kingdom

OLUREMI A. OLATUNBOSUN: O.A.Olatunbosun@bham.ac.uk
School of Mechanical Engineering, The University of Birmingham, Edgbaston, Birmingham B15 2TT, United Kingdom